TWIST AND NON–TWIST REGIMES OF THE OBLATE PLANET PROBLEM

ALESSANDRA CELLETTI, FABRIZIO PAITA, AND GIUSEPPE PUCACCO

ABSTRACT. We consider the dynamics of a point-mass object, e.g. a small satellite, around a primary rigid body, e.g. a planet. We assume that the planet is oblate and axially symmetric with respect to the vertical axis. Revisiting a procedure described in [19], we make use of the first integrals (the energy and the projection of the angular momentum on the vertical axis), so to reduce the problem to the study of a one-dimensional, time-dependent Hamiltonian system. Such Hamiltonian depends upon control parameters, which represent the coefficients of the zonal terms of the gravitational potential. We provide the explicit expressions of the most relevant terms of the expansion of the potential in spherical harmonics. Averaging over the fast angles one obtains a one-dimensional system. A Poincaré map of such Hamiltonian is also introduced. We discuss the conditions under which the Hamiltonian (or the mapping) satisfies the twist condition, which is needed in KAM theory to ensure the existence of rotational invariant surfaces. A qualitative description of the dynamics in the twist and non-twist regimes is performed; it is based on the analysis of the equilibrium solutions and on the occurrence of bifurcations as the parameters are varied.

Alla memoria del Prof. Giuseppe Grioli

1. Introduction

A reliable formulation of satellite dynamics requires the introduction of a model in which the central body is not considered just as

2010 *Mathematics Subject Classification.* 37N05, 70E20, 70K50.

Key words and phrases. Rigid body, Oblate planet problem, Non-twist map, Bifurcation.

This work was partially supported by the Italian Space Agency - ASI under the contract 2013-056-RO for JUICE phase A/B1 and by GNFM/INdAM.

a point-mass. Therefore, it is convenient to assume that the central object, hereafter the *planet,* is a rigid body with oblate shape and axial symmetry with respect to the vertical axis. We assume that the satellite and the planet interact just through the gravitational force and we neglect the influence due to other bodies as well as tidal torques that may arise from the non-rigidity of the planet. The model which describes the *oblate planet problem* is governed by a Hamiltonian function, which can be conveniently expressed in terms of the Delaunay action-angle variables (see, e.g., [3]). According to a procedure described in [19] (see also [13], [18], [23], [24]), the Hamiltonian can be reduced by using the first integrals of motion given by the energy and the projection of the angular momentum on the vertical axis. Using such integrals and averaging over the fast angle (i.e., the mean anomaly), one is led to consider a one-dimensional, time-dependent Hamiltonian function in action-angle variables, where the action G is related to the eccentricity of the orbit, while the angle g represents the argument of perigee. Correspondingly, one can introduce a discrete mapping as the Poincaré map of the Hamiltonian at multiples of 2π.

The averaged reduced Hamiltonian can be decomposed in the form (compare with (2.12) below)

$$\overline{K}(G, g; \widetilde{L}, H) = K_0(G; H) + \varepsilon K_1(G, g; \widetilde{L}, H) \ ,$$

where $\widetilde{L}$, H are the first integrals, K_0 represents the integrable Hamiltonian, K_1 is the perturbing function which is multiplied by a parameter ε (depending on the so-called *zonal coefficients* J_k of the gravitational potential), that we assume to be small ([17]). If only J_2 is considered, then the problem is usually called the *J_2-problem.*

The oblate planet problem (or its variant - the J_2-problem) can be used for the description of the artificial satellite dynamics, but it has also received attention in various contexts, since it has been analyzed as a bench test of different aspects in Dynamical Systems and Astrodynamics. Most notably, we mention the use of this model in connection to the proof of its non-integrability based on Lerman ([8]) or Ziglin ([16]) theorems, the global structure of the reduced phase space ([10]), the analysis of collision orbits ([22]), the investigation of periodic solutions ([4, 18, 19]). Particular values of a control parameter (the inclination) lead to a model which paves the way to the study of the non-twist dynamics that has been carefully investigated in different examples (see, e.g., [11, 26, 29, 31]. Finally, an application of KAM theory is given, e.g., in [19] by applying Moser's small twist theorem; the oblate planet model is also taken as an appropriate example to prove the existence of invariant curves within the non-twist regime (see, e.g., [12, 15]).

Rather than being interested in the orbital propagation of the satellite, we concentrate on the qualitative and geometrical aspects of the model, especially by looking at the behavior of the dynamics as some control parameters are varied. In particular, we analyze the problem under non-degenerate and degenerate conditions, precisely the twist and non-twist conditions (see, e.g., [11, 12, 26, 27, 29]), and in such cases we study the occurrence of bifurcations of equilibria (see, e.g., [7, 14, 28]).

To be more precise, we analyze the oblate plane model when a relevant quantity, represented by the second derivative of the unperturbed Hamiltonian, is varied. Precisely, when such derivative is different from zero, the system is *non-degenerate* or, equivalently, the Poincaré map satisfies the *twist* condition; for the values at which such derivative is zero, we say that the system is *degenerate* or that the map is *non-twist*. Non-degeneracy and twist conditions are required to prove the celebrated Kolmogorov-Arnold-Moser (hereafter, KAM) theorem ([20], [1], [25]), which allows one to show the existence of rotational invariant surfaces, with the property that they are graphs over the angle coordinate. It can be easily shown that the oblate planet problem becomes non-twist at specific values of the inclination. For such values, the dynamics presents a behavior quite different from the twist case, with the occurrence of so-called *meandering* tori, which are not graphs over the angle variables.

Beside showing twist and non-twist behaviors, the model we consider offers also another interesting feature, precisely the occurrence of bifurcations of equilibria as a control parameter is varied: in the present setting, the role of control parameter is played by the asymmetric coefficient J_3. By varying this parameter, we observe the birth or annihilation of periodic orbits, either in the twist and non-twist regimes. In summary, due to its twofold intrinsic interest, we propose the oblate planet problem as a paradigmatic model in which it is possible to study two different interrelated aspects: the twist/non-twist regimes and the occurrence of bifurcations.

This paper is organized as follows. In Section 2 we revisit the method used in [19] to introduce the oblate planet model and we give an explicit approximated expression of the potential; we also discuss the twist condition as a function of the orbital elements. In Section 3 we draw some conclusions on the existence of invariant surfaces. A qualitative description of the dynamics is provided in Section 4, where we compute the equilibrium positions and we analyze bifurcation phenomena as the control parameters are varied.

2. The oblate planet model

We consider a satellite subject to the gravitational influence of a rigid oblate planet. We assume that the mass of the satellite is negligible with respect to that of the planet (for example, the satellite is a spacecraft). After introducing the potential function in Section 2.1, we revisit a method described in [19], which allows us to reduce the equations of motion to a one-dimensional, time-dependent Hamiltonian model. The method makes use of the first integrals of motion, namely the energy and the projection of the angular momentum on the vertical axis. Then, the equations of motion are conveniently expressed in terms of the mean anomaly (Section 2.2); such equations can be integrated over a period to obtain the Poincaré map (see Section 2.3). In particular, we consider the system (and the map) obtained after averaging over the fast variable (see Section 2.4). The twist properties of such mapping are discussed in Section 2.5.

2.1. The potential.

Let us consider an inertial reference frame (O, x, y, z), whose origin coincides with the center of mass of the planet, the z axis is aligned with the polar axis, while the x and y axes lie on the equatorial plane to form an oriented frame. Denoting by $\vec{r}$ and $\vec{v}$ the position and velocity vectors of the satellite, we have

$$\frac{d\vec{r}}{dt} = \vec{v} \ , \qquad \frac{d\vec{v}}{dt} = -\nabla V \ ,$$

where V denotes the potential energy. We assume that the planet is axially symmetric with respect to the z axis. Thanks to this assumption, the potential energy $V = V(x, y, z)$ can be expanded in terms of the Legendre polynomials as

$$V\,(x, y, z) = -\frac{\mu}{r} + \mu \ \sum_{j=2}^{\infty} J_j \frac{R_e}{r^{j+1}} P_j\left(\frac{z}{r}\right) , \tag{2.1}$$

where $r = r(x, y, z)$ is the Euclidean norm of $\vec{r}$, $\mu \equiv kM$ is taken in normalized units (k denotes the gravitational constant, while M stands for the mass of the planet) and R_e is the equatorial radius of the planet. We normalize the units of distance so that $R_e = 1$. The quantities J_j in (2.1) are constants which depend on the mass distribution of the planet, while the functions P_j are the Legendre polynomials of degree j. The term corresponding to $j = 1$ in the series expansion (2.1) is missing, due to the fact that the center of mass of the planet coincides with the origin of the inertial frame. Since the planet is not spherically symmetric, the angular momentum is not constant. However, assuming axial symmetry of the planet, the projection H of the angular momentum on the z axis is constant. Another integral of motion is given by the total energy $\widetilde{H}$, which is assumed to be negative, thus providing bounded unperturbed trajectories. No other integral of motion can be determined, except for particular choices of the coefficients J_j; for example, when $J_j = 0$ for any j, then the model reduces to Kepler's problem. Next, we write (2.1) as

$$V(x, y, z) = U_{Kep}(x, y, z) + U(x, y, z) \ ,$$

where the Keplerian potential is $U_{Kep} = -\frac{\mu}{r}$ and we have introduced the *perturbative* potential given by

$$U\left(x, y, z\right) \equiv -\mu \sum_{j=2}^{\infty} J_j \frac{1}{r^{j+1}} P_j \left(\frac{z}{r}\right) \ . \tag{2.2}$$

2.2. **A reduced system of equations.** We denote the orbital elements as follows: a is the semimajor axis, e the eccentricity, i the inclination, ℓ the mean anomaly, g the argument of perigee and h the longitude of the ascending node. Setting n the mean motion, according to Kepler's third law, we have $n^2 a^3 = \mu$.

Following [19], we make use of the first integrals to describe the oblate planet model by a non–autonomous, one–dimensional Hamiltonian function. To this end, we introduce the Delaunay action variables defined in terms of the orbital elements as

$$L = (\mu a)^{\frac{1}{2}} \ , \quad G = L\left(1-e^2\right)^{\frac{1}{2}} \ , \quad H = G\cos i \ , \tag{2.3}$$

while the conjugated angles are ℓ, g, h. We notice that H represents the integral given by the projection of the angular momentum on the vertical axis, while the energy coincides with the Hamiltonian function, that we express as

$$\widetilde{H}(L,G,H,\ell,g) = -\frac{\mu^2}{2L^2} - U\left(L,G,H,\ell,g\right) \ , \tag{2.4}$$

where the function U in (2.2) is now expressed in terms of the Delaunay variables. We fix the integrals as $H = \alpha$ for some $\alpha \in \mathbb{R}$, $\widetilde{H} = \beta$ for some $\beta \in \mathbb{R}$. Following [19], we solve the equation $\widetilde{H}(L,G,\alpha,\ell,g) = \beta$ to obtain $L = \widetilde{K}(G,\alpha,\ell,g,\beta)$ for some function $\widetilde{K}$, so that we can consider the Hamiltonian $\widetilde{H}$ as depending just on G, ℓ, g and parametrized by α, β.

Finally, we consider ℓ instead of t as an independent variable to obtain the equations

$$\frac{dg}{d\ell} = \frac{\frac{\partial \widetilde{H}}{\partial G}}{\frac{\partial \widetilde{H}}{\partial L}} \ , \qquad \frac{dG}{d\ell} = -\frac{\frac{\partial \widetilde{H}}{\partial g}}{\frac{\partial \widetilde{H}}{\partial L}} \ , \tag{2.5}$$

where $\widetilde{H} = \widetilde{H}\left(\widetilde{K}\left(G,\alpha,\ell,g,\beta\right),G,\alpha,\ell,g\right)$. The final step consists in differentiating $\widetilde{H}\left(\widetilde{K}\left(G,\alpha,\ell,g,\beta\right),G,\alpha,\ell,g\right) = \beta$ with respect to the variables G and g to obtain

$$\frac{\partial \widetilde{H}}{\partial L}\frac{\partial \widetilde{K}}{\partial G} + \frac{\partial \widetilde{H}}{\partial G} = 0 \ , \qquad \frac{\partial \widetilde{H}}{\partial L}\frac{\partial \widetilde{K}}{\partial g} + \frac{\partial \widetilde{H}}{\partial g} = 0 \ . \tag{2.6}$$

Setting

$$K(G,g,\ell;\alpha,\beta) \equiv \widetilde{K}(G,\alpha,\ell,g,\beta) - \frac{\mu}{(-2\beta)^{\frac{1}{2}}} \tag{2.7}$$

and using (2.5), (2.6), we obtain

$$\frac{dg}{d\ell} = -\frac{\partial K(G,g,\ell;\alpha,\beta)}{\partial G}\ , \qquad \frac{dG}{d\ell} = \frac{\partial K(G,g,\ell;\alpha,\beta)}{\partial g}\ . \tag{2.8}$$

We remark that the quantities α, β cannot be arbitrary, but they must satisfy the inequalities

$$0 \leq \alpha \leq \frac{\mu}{(-2\beta)^{\frac{1}{2}}}\ .$$

2.3. **The Poincaré map.** Let us introduce a new variable $\widetilde{L}$ through the equation $-\beta = \mu^2/2\widetilde{L}^2$. By using the energy integral and the Hamiltonian defined by the equation (2.4), we get

$$\frac{\mu^2}{2\widetilde{L}^2} = \frac{\mu^2}{2L^2} + U\left(L,G,\ell,g,\alpha\right)\ ,$$

that we can invert to obtain L in terms of $\widetilde{L}$, hence of β. Following [18], we can reduce to the study of the Poincaré mapping associated to (2.8), described by the equations

$$\begin{aligned} G(2\pi) &= G(0) + \int_0^{2\pi} \frac{\partial K}{\partial g}\left(G(\ell),g(\ell),\ell;\alpha,\beta\right) d\ell \\ g(2\pi) &= g(0) - \int_0^{2\pi} \frac{\partial K}{\partial G}\left(G(\ell),g(\ell),\ell;\alpha,\beta\right) d\ell\ , \end{aligned} \tag{2.9}$$

where $(G(0),g(0))$ denote the initial conditions. Given the dependence of K on the variables (G,g,ℓ), we need to express U in terms of such variables, as described in the following section where an averaged approximation of the potential is considered.

2.4. **The averaged problem.** Due to the assumption of axial symmetry, we limit to consider the so–called *zonal* harmonics in the expansion of the potential ([2]). Therefore, U in (2.2) can be written as $U = V_{20} + V_{30} + ...$, where the terms V_{j0} are defined by

$$V_{j0} = \frac{\mu}{a(\widetilde{L})^{j+1}} \sum_{p=0}^{j} \mathcal{F}_{j0p}\left(i\left(G,H\right)\right) \sum_{q=-\infty}^{\infty} \mathcal{G}_{jpq}(e(G,\widetilde{L}))\mathcal{H}_{j0pq}\left(g,\ell\right) \ , \tag{2.10}$$

where $a = a(\widetilde{L}) = \widetilde{L}^2/\mu$, $e = e(G,\widetilde{L}) = \sqrt{1 - G^2/\widetilde{L}^2}$, $i = i\left(G,H\right) = \arccos\left(H/G\right)$, while the expressions of the functions $\mathcal{F}_{jmp}$, $\mathcal{G}_{jpq}$, $\mathcal{H}_{jmpq}$ are recalled in Appendix A.

In the expansion (2.10) we consider only the terms with $q = 2p - j$, since we are just interested to terms of U with zero average with respect to ℓ. After tedious computations, we obtain the following expressions for V_{20} and V_{30}, which provide the potential U truncated to the first two terms, namely $U = V_{20} + V_{30}$ with

$$\begin{aligned} V_{20} &= J_2 \mu^4 \widetilde{L}^{-3} G^{-3} \left(\frac{3}{4}\frac{H^2}{G^2} - \frac{1}{4} \right) \ , \\ V_{30} &= 2\ J_3 \mu^5 \widetilde{L}^{-3} G^{-5} \sin\left(g\right) \left(\frac{15}{16}\frac{H^2}{G^2} - \frac{3}{16} \right) \left(1 - \frac{H^2}{G^2} - \frac{G^2}{\widetilde{L}^2} + \frac{H^2}{\widetilde{L}^2} \right)^{\frac{1}{2}} \ . \end{aligned} \tag{2.11}$$

Notice that the secular terms appear only in the functions V_{j0} with j even. From the relations (2.7) and (2.11), we obtain the following expression for the Hamiltonian $\overline{K}$, averaged with respect to ℓ:

$$\begin{aligned} &\overline{K}(G,g;\widetilde{L},H) = J_2 \mu^2 G^{-3} \left(\frac{3}{4}\frac{H^2}{G^2} - \frac{1}{4} \right) \\ &+ 2\ J_3 \mu^3 G^{-5} \sin\left(g\right) \left(\frac{15}{16}\frac{H^2}{G^2} - \frac{3}{16} \right) \left(1 - \frac{H^2}{G^2} - \frac{G^2}{\widetilde{L}^2} + \frac{H^2}{\widetilde{L}^2} \right)^{\frac{1}{2}} \ . \end{aligned} \tag{2.12}$$

Finally, we can give an explicit form to the Poincaré map (2.9) associated to the averaged model and we can introduce the following map $\mathcal{M} : \mathbb{R} \times \mathbb{T} \to \mathbb{R} \times \mathbb{T}$ truncated up to first order in J_3, where G_0, g_0 denote the solutions at time $t = 0$, while G_1, g_1 are the solutions at $t = 2\pi$:

$$\begin{aligned} G_1 &= G_0 + 2\pi J_3 \; F_g\left(G_0, g_0\right) \\ g_1 &= g_0 - 2\pi \left[J_2 \gamma\left(G_1\right) + J_3 F_G\left(G_1, g_0\right)\right] \; ; \end{aligned} \tag{2.13}$$

in the above expressions, the functions γ, F_g and F_G are defined by following the relations:

$$\gamma(G_1) = \frac{3}{4}\,\frac{\mu^2}{G_1^4}(1 - 5\frac{H^2}{G_1^2}) \; , \tag{2.14}$$

$$F_g\left(G_0, g_0\right) = 2\,\mu^3 G_0^{-5} \cos\left(g_0\right) \frac{3}{16}\left(5\frac{H^2}{G_0^2} - 1\right)\left(1 - \frac{H^2}{G_0^2} - \frac{G_0^2}{\widetilde{L}^2} + \frac{H^2}{\widetilde{L}^2}\right)^{\frac{1}{2}} \tag{2.15}$$

and

$$F_G\left(G_1, g_0\right) = 2\,\mu^3 \sin\left(g_0\right)\left(\frac{15}{16}\frac{1}{G_1^6} - \frac{105}{16}\frac{H^2}{G_1^8}\right)\left(1 - \frac{H^2}{G_1^2} - \frac{G_1^2}{\widetilde{L}^2} + \frac{H^2}{\widetilde{L}^2}\right)^{\frac{1}{2}}$$
$$+ 2\,\mu^3 \sin\left(g_0\right)\left(\frac{15}{16}\frac{H^2}{G_1^7} - \frac{3}{16}\frac{1}{G_1^5}\right)\left(1 - \frac{H^2}{G_1^2} - \frac{G_1^2}{\widetilde{L}^2} + \frac{H^2}{\widetilde{L}^2}\right)^{-\frac{1}{2}}\left(\frac{H^2}{G_1^3} - \frac{G_1}{\widetilde{L}^2}\right) \; .$$

Remark 1. *We underline that in the second equation of* (2.13) *we have inserted the iterated value of the G–variable, say G_1; this allows to obtain a better preservation of the area of the mapping $\mathcal{M}$ up to $O(J_3^2)$, as it can be easily checked by computing the determinant of the Jacobian of the mapping.*

2.5. **The twist condition.** An important feature of the map (2.13) is the behavior of the function (2.14). Precisely, the map is said to satisfy the *twist condition,* if $\gamma'(G) > 0$ in the domain where the map is considered. Such condition is an essential requirement for the application of KAM theory ([20], [1], [25]) on the existence of invariant curves (see Section 3). On the other hand, maps which do not satisfy the twist condition admit a peculiar dynamics, which includes curves which are not graphs (the so-called *meandering* curves). Note that, in the following computation instead of considering the iterated value G_1 for the variable G in the equation for g (compare with Remark 1), we consider the original variable G_0 (see also Remark 2 below). Given the expression (2.14) with G_0 in place of G_1, we have

$$\gamma'\left(G_0\right) = \frac{3}{2}\frac{\mu^2}{G_0^5}(2 - 15\frac{H^2}{G_0^2}) \ . \tag{2.16}$$

We say that the map $\mathcal{M}$ satisfies the twist condition, if G_0 is such that

$$\gamma'(G_0) \neq 0 \ . \tag{2.17}$$

As already remarked in [19], the twist condition is violated for $\gamma'(G_0) = 0$, namely whenever $H^2/G_0^2 = 2/15$ or $\cos^2 i = 2/15$, which holds for $i = 68^o.583$ or $i = 111^o.417$; we shall refer to such values as the *non–twist inclinations.* As we shall see in Section 3, we need to exclude such critical values in order to guarantee the persistence of rotational invariant curves by means of KAM theory.

Remark 2. *The twist quantity* (2.16) *was obtained by assuming in* (2.14) *to have the function at G_0 and not at G_1. If instead we consider $\gamma = \gamma(G_1)$ with G_1 as a function of G_0 through the first of* (2.13)*, we obtain:*

$$\frac{\partial}{\partial G_0}\left[\gamma\left(G_1\left(G_0\right)\right)\right] = \frac{\partial}{\partial G_1}\left[\gamma\left(G_1\left(G_0\right)\right)\right]\left(1 + 2\pi J_3\ \frac{\partial}{\partial G_0}\left[F_g\left(G_0, g_0\right)\right]\right) \ ,$$

where

$$\frac{\partial}{\partial G_1}\left[\gamma\left(G_1\left(G_0\right)\right)\right] = \frac{3}{2}\frac{\mu^2}{G_1^5}(2 - 15\frac{H^2}{G_1^2}) \tag{2.18}$$

and

$$\frac{\partial}{\partial G_0}\left[F_g\left(G_0,g_0\right)\right]=$$

$$=2\mu^3\cos(g_0)\left(\frac{15}{16}\frac{1}{G_0^6}-\frac{105}{16}\frac{H^2}{G_0^8}\right)\left(1-\frac{H^2}{G_0^2}-\frac{G_0^2}{\tilde{L}^2}+\frac{H^2}{\tilde{L}^2}\right)^{\frac{1}{2}}$$

$$+\,2\mu^3\cos(g_0)\left(\frac{15}{16}\frac{H^2}{G_0^7}-\frac{3}{16}\frac{1}{G_0^5}\right)\left(1-\frac{H^2}{G_0^2}-\frac{G_0^2}{\tilde{L}^2}+\frac{H^2}{\tilde{L}^2}\right)^{-\frac{1}{2}}\left(\frac{H^2}{G_0^3}-\frac{G_0}{\tilde{L}^2}\right).$$

Note that, since we used the iterated variable G_1 in (2.14) *and since we considered the expression of the oblate potential up to orders proportional to J_3, the expression of the twist functions* (2.16) *and* (2.18) *differ slightly (as far as J_3 is small). However, since the quantities in* (2.14) *and* (2.15) *are zero for the same values of the initial inclination, this means that the same happens for the quantities in* (2.14) *and* (2.18)*.*

3. Invariant curves

The model described by (2.12), or equivalently (2.13), shows different features, according to whether the twist or non-twist condition is satisfied. Under the assumption that (2.17) holds, then we can find KAM invariant curves, which are characterized by a frequency satisfying the Diophantine condition. Precisely, let us consider the mapping $\mathcal{M}$ in (2.13), defined on a manifold $\mathcal{D}\equiv V\times\mathbb{T}$ with $V\subset\mathbb{R}$ open. We assume that the frequency ω satisfies the Diophantine condition

$$|\frac{\omega}{2\pi}\,q+p|^{-1}\leq\nu\,|q|^{\tau}\ ,\qquad p\in\mathbb{Z}\ ,\quad q\in\mathbb{Z}\backslash\{0\}$$

for some $\nu\geq 1$, $\tau\geq 1$. Then, we have the following definition of KAM invariant curve.

Definition 3. *A KAM curve for* (2.13) *with Diophantine frequency ω is an invariant curve, described parametrically by an embedding P :*

$\mathbb{T} \to \mathcal{D}$, *which satisfies the invariance equation*

$$\mathcal{M} \circ P(\theta) = P(\theta + \omega) \ . \tag{3.1}$$

Provided that the twist condition is satisfied, then for suitable values of the parameters we have plenty of KAM rotational curves, whose existence is guaranteed by KAM theory ([20], [1], [25], see also [21], [6] and references therein). Following the proof described in [21], the existence of KAM manifolds can be shown using an a-posteriori approach. In short, starting with an approximate solution P_0 which satisfies the invariance equation (3.1) up to an error term $E_0 = E_0(\theta)$, say

$$\mathcal{M} \circ P_0(\theta) - P_0(\theta + \omega) = E_0(\theta) \ ,$$

assuming the twist condition (2.17), if the norm of E_0 is sufficiently small, then there exists a solution P_e which satisfies (3.1) exactly and such that the norm of $P_e - P_0$ (on a smaller domain compared to the domain on which P_0 is defined) is bounded by the norm of E_0, multiplied by suitable powers of the Diophantine constant ν and by the inverse of the parameter which measures the domain loss. We refer to [21] for complete details (see also [5] for an extension of the proof to some dissipative systems, like the case of a satellite around an oblate primary and subject to a tidal torque).

An important consequence of the KAM theory within the present model is that, by proving the existence of two invariant curves, we obtain a confinement between those invariant manifolds. In fact, any motion between any two invariant curves will always remain trapped between the invariant manifolds. Notice that due to (2.3) such confinement is indeed a bound on the eccentricity between the values corresponding to the trapping invariant curves.

When the non-twist condition is violated, we have the appearance of different phenomena (see, e.g., [11], [14]). For example, there might exist several rotational invariant curves and periodic orbits with the same frequency. Then, it might happen that a parameter change gives rise to bifurcations of orbits with the same frequency, which generate either a collision, an annihilation or rather a separatrix reconnection. For example, in the integrable case $J_3 = 0$, it is clear that the invariant curves $G = \pm G_0$ have the same frequency. As it is well known, non-twist maps exhibit also the appearance of *meandering* curves, which are characterized by the fact that they are not graphs over the angle variable. Some of these phenomena will appear in the qualitative description provided in Section 4. We refer to [11], [26], [28], [31], [29], [30], and references therein, for further details. For a formulation of KAM theory for non-twist maps we refer, e.g., to [12], [15], [27].

4. Equilibrium solutions and bifurcations

In this Section we perform a qualitative analysis of the model described in Section 2. First, we determine the equilibrium solutions (see Section 4.1), which are characterized by a constant value of the eccentricity and the argument of perihelion. Equilibrium profiles associated to the mapping (2.13) allow us to determine the location of the equilibria and their evolution as the parameters are varied (see Section 4.2). This analysis is further complemented and widened by a study of the bifurcations of the equilibria, which is performed in Section 4.3.

4.1. **Equilibrium solutions.**

With reference to the mapping (2.13), we proceed to compute the equilibrium points of the mapping, which correspond to the solutions in which (G, g) are invariant, namely the eccentricity and the argument of perihelion stay constant under the effect of the J_2 and J_3 terms. This kind of trajectories are known in satellite dynamics as *frozen orbits* ([9]).

i) We observe that for $G_0 = \overline{G}_0 = \sqrt{5}\alpha$ we obtain $F_g(\overline{G}_0, g_0) = 0$ for any value of g_0. This solution implies that $G_1 = G_0$ and that $\gamma(\overline{G}_1) = 0$. The condition on $\overline{G}_0$ means that the inclination takes the values $i = 63^o.435$ or $i = 116^o.565$, to which we will refer as the *critical inclination* values. To have the invariance of the angular variable, we need to require that $F_G(\overline{G}_0, g_0) = 0$, which is satisfied for $g_0 = 0$ or $g_0 = \pi$. In conclusion, we obtain the following equilibrium points:

$$\begin{aligned} \overline{G}_0 &= \sqrt{5}\alpha \ , \qquad g_0 = 0 \\ \overline{G}_0 &= \sqrt{5}\alpha \ , \qquad g_0 = \pi \ . \end{aligned}$$

ii) Another equilibrium solution is obtained as follows. We observe that for $g_- = \frac{\pi}{2}$ and $g_+ = \frac{3}{2}\pi$ we obtain $F_g(G_0, g_\pm) = 0$, which implies that the action variable is kept fixed. On the other hand, we look for the values of G_1 (equivalently, G_0), such that

$$J_2\gamma(G_1) + J_3 F_G(G_1, g_\pm) = 0 \ . \tag{4.1}$$

The solutions (not necessarily unique) of (4.1) determine the equilibrium points of the mapping (2.13). Notice that the equation (4.1) provides a relation between the eccentricity, the inclination and the semimajor axis.

4.2. **Equilibrium profiles.** We can infer several information from the graph of the function

$$\mathcal{F}(G_1, g_0) = -J_2\gamma\,(G_1) - J_3 F_G\,(G_1, g_0) \tag{4.2}$$

computed, for example, at the equilibrium position $g_0 = \frac{3}{2}\pi$ and for fixed values of the quantities $\widetilde{L}$, H. The zeros of $\mathcal{F}(G_1, \frac{3}{2}\pi)$ provide the values of the action, corresponding to the equilibrium solution

$g_0 = \frac{3}{2}\pi$. In Figure 1 we fix a value for J_2 and we let the parameter J_3 increase, plotting the most significant cases:

(1) a transverse intersection with the horizontal axis (Figure 1, left panel) corresponds to a single equilibrium point;
(2) a tangency, as in the middle panel of Figure 1, corresponds to a case where the bifurcation threshold is reached;
(3) for higher values of J_3, there appear three equilibria (right panel of Figure 1).

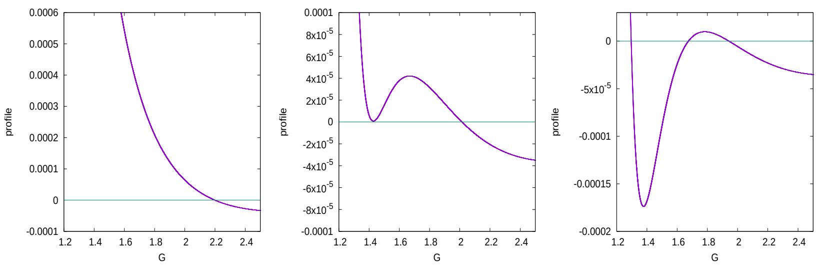

FIGURE 1. Equilibrium profiles for $\widetilde{L} = 3$, $G_0 = 2.8$, $H = G_0\sqrt{\frac{2}{15}}$, $J_2 = 10^{-2}$; left: $J_3 = 5 \cdot 10^{-3}$, middle: $J_3 = 8.83 \cdot 10^{-3}$, right: $J_3 = 9.3 \cdot 10^{-3}$.

This analysis, which is quite easy and computationally fast, provides a very good indication of the equilibrium positions, as it will be confirmed by a more elaborated study presented in the next section.

4.3. **Bifurcation theory for a one degree-of-freedom system.** For a Hamiltonian system, low-dimensional invariant manifolds (either equilibria, periodic orbits or invariant tori) organize the structure of the phase space. For one degree-of-freedom systems, the critical points of the Hamiltonian function identify the equilibria and the invariant manifolds associated to the phase flow coincide with the level curves of the Hamiltonian. In the case in which this Hamiltonian stems from a reduction procedure associated to the existence of one or more integrals of motion, the equilibria correspond to periodic orbits and the invariant curves to tori of the un-reduced system. The number and nature of the critical points, as they are determined by varying intrinsic and control parameters, provide information about bifurcation phenomena, with either the birth or the annihilation of periodic orbits. We start with a Hamiltonian as in (2.12), say $\overline{K} = \overline{K}(G, g; \widetilde{L}, H; J_2, J_3)$ in the phase-plane (G, g), where $\widetilde{L}$, H are the intrinsic parameters and J_2, J_3 the control ones but, since J_3 determines the magnitude of the angle-dependent term, it plays the role of perturbation control parameter. The variable G is limited by $G_{min} \leq G \leq L$, where G_{min} can be zero or it can be determined by some physical constraints (see [7]). Therefore, the available phase-space of the Hamiltonian system is represented by the cylinder

$$\Gamma \equiv \{(G, g) \in \mathbb{R} \times \mathbb{T} : \; G_{min} \leq G \leq L \; , \quad 0 \leq g \leq 2\pi\} \; .$$

Whenever the perturbation parameter J_3 is small, the flow in Γ is a *rotational* set of lines almost parallel to the base of the cylinder $G = G_{min}$. Depending on the extent of the perturbation and the value of the internal parameters $\widetilde{L}$, H, critical points may appear in Γ: this leads to the birth of *libration islands* and, in case, to the appearance of stable and unstable manifolds. As mentioned in Section 4.1, to find the critical points we have to solve the system of equations

$$\frac{\partial \overline{K}}{\partial G} = 0 \; , \qquad \frac{\partial \overline{K}}{\partial g} = 0 \; . \tag{4.3}$$

The second equation is readily solved by $g_- = \pi/2$ and $g_+ = 3/2\pi$. These two pairs of solutions, when inserted in the first of (4.3), give the two equations:

$$\mathcal{F}_\pm(G) = 0 \tag{4.4}$$

with $\mathcal{F}_\pm(G) = \mathcal{F}(G, g_\pm)$ and $\mathcal{F}$ as in (4.2). Then, we need to find the roots of this pair of equations as functions of the parameters. Two kind of bifurcation phenomena may happen:

(1) every time one of the roots enters into the cylinder Γ by varying the parameters, we have a new equilibrium of the reduced problem (a periodic orbit in the original system), whose stable or unstable nature can be assessed by studying the Hessian of the Hamiltonian;
(2) at critical values of the parameters, the number of roots may change, giving rise to the birth (or annihilation) of new critical points.

Remark 4. *The explicit solution of* (4.4) *is easy to find when the equations are linear or quadratic in G. For higher order or non-polynomial equations, usually the presence of a small perturbation parameter allows the determination of approximate solutions.*

We present in Figure 2 an example of the computation of the contour plots of the Hamiltonian (2.12), from which we infer the existence of different equilibria and the occurrence of bifurcations. Moreover, for small values of the perturbing parameter J_3 we can compute analytically the values of the action G, which correspond to the equilibrium solutions. The procedure is the following. Let $G_0 = \sqrt{5}H$ as above and let $g_- = \pi/2$, $g_+ = 3/2\pi$ be the values of g at the equilibria. Let us decompose $\overline{K}$ in (2.12) as $\overline{K}(G, g; \widetilde{L}, H) = K_1(G; \widetilde{L}, H) + K_2(G, g; \widetilde{L}, H)$, where K_1 is the part proportional to J_2 and K_2 the term proportional to J_3. To find an approximate value of the root, we can apply the Newton-Raphson method. Precisely, we start by defining the quantities

$$\eta_\pm \equiv -\frac{\frac{\partial K_2(G_0, g_\pm)}{\partial G}}{\frac{\partial^2 K_1(G_0)}{\partial G^2}} \ .$$

Then, the first-order (in J_3) approximate solutions are given by

$$G_\pm = G_0 + \eta_\pm$$

or, explicitly in terms of the parameters,

$$G_\pm = \sqrt{5}H \pm \frac{J_3}{J_2}\frac{\sqrt{1-5(H/L)^2}}{5H}\ . \tag{4.5}$$

The horizontal lines in the upper plots of Figure 2 correspond to the values $G_\pm$ computed as in (4.5).

In particular, in the upper left plot of Figure 2 we have two stable equilibria, whose action values lie on the lines $G_\pm$, although the prediction of the ordinate of the equilibria becomes less reliable as the parameter J_3 increases (compare with the upper right plot of Figure 2). At $J_3 = 5 \cdot 10^{-3}$ we still have a pair of equilibria (Figure 2, middle left panel), but the tori below the lower equilibrium become more and more distorted as J_3 increases (middle right panel of Figure 2), until a bifurcation value is reached and more equilibria appear. They are produced in a *saddle–centre* bifurcation occurring at the bifurcation value $J_3 = 8.83 \cdot 10^{-3}$ as shown in the lower left panel of Figure 2. We notice that for such value of J_3 there appear meandering curves, typical of the non-twist regime, around the equilibria at $g_+ = 3/2\pi$. The stable-unstable pair of critical points displayed in the lower right panel of Figure 2 shows the behavior for a non critical value of the parameters, precisely for $H = 0.5$ and $J_3 = 10^{-3}$. We highlight that Figure 2 presents two important phenomena typical of some dynamical systems, precisely the transition from a twist to a non-twist regime and the occurrence of bifurcations with the birth of new equilibria. Unfortunately, it is not possible to provide an approximate analytical expression for the additional roots associated to the bifurcation and, as a consequence, the estimate of the threshold value of J_3 has only been obtained numerically. The reason stays in the breakdown of the Newton-Raphson procedure for which is not possible to identify a sensible seed solution.

A. Appendix: The gravitational potential

In polar coordinates (r, ϕ, λ) with origin at the center of mass of the planet, the real solution of the Laplace equation $r^2 \nabla^2 V(r, \phi, \lambda) = 0$ is given by

$$\begin{aligned} V(r,\phi,\lambda) &= \sum_{j,m} V_{jm}(r,\phi,\lambda) \\ &= \sum_{j=0}^{\infty} \sum_{m=0}^{j} \frac{\mu}{r^{j+1}} P_{jm}\left(\sin\left(\phi\right)\right)\left[C_{jm}\cos\left(m\lambda\right) + S_{jm}\sin\left(m\lambda\right)\right] \ . \end{aligned} \tag{A.1}$$

The quantities $P_{jm}\left(\sin\left(\phi\right)\right)$ are the Legendre associate functions, defined as

$$P_{jm}\left(\sin\left(\phi\right)\right) = \cos^m\left(\phi\right) \sum_{t=0}^{\left[\frac{j-m}{2}\right]} T_{jmt} \sin^{j-m-2t}\left(\phi\right),$$

where the coefficients T_{jmt} are given by

$$T_{jmt} = \frac{(-1)^t\,(2j-2t)!}{2^j t!\,(j-t)!\,(j-m-2t)!} \ .$$

The constants C_{jm} and S_{jm} in (A.1) depend on the mass distribution of the planet (see [17]). In particular, one has $C_{i0} = -J_i$, where J_i denote the coefficients entering the potential (2.2). It is convenient to write the potential (A.1) using the orbital elements (a, e, i, ℓ, g, h) as in [17]:

$$V_{jm} = \mu \frac{R_e^j}{a^{j+1}} \sum_{p=0}^{j} \mathcal{F}_{jmp}\left(i\right) \sum_{q=-\infty}^{\infty} \mathcal{G}_{jpq}\left(e\right) \mathcal{H}_{jmpq}\left(\ell, g, h, \theta\right),$$

where θ denotes the sidereal time and R_e is the equatorial radius of the planet. The quantities $\mathcal{H}_{jmpq}$ are defined as

$$\begin{aligned}\mathcal{H}_{jmpq}(\ell,g,h,\theta) = C_{jm}&\left[\cos\Big(\,(j-2p)\,g+(j-2p+q)\,\ell+m\,(h-\theta)\Big)\right]\\ +\,S_{jm}&\left[\sin\Big(\,(j-2p)\,g+(j-2p+q)\,\ell+m\,(h-\theta)\Big)\right]\end{aligned}$$

if $j-m$ is even, or

$$\begin{aligned}\mathcal{H}_{jmpq}(\ell,g,h,\theta) = -S_{jm}&\left[\cos\Big(\,(j-2p)\,g+(j-2p+q)\,\ell+m\,(h-\theta)\Big)\right]\\ +\,C_{jm}&\left[\sin\Big(\,(j-2p)\,g+(j-2p+q)\,\ell+m\,(h-\theta)\Big)\right]\end{aligned}$$

if $j-m$ is odd. The expressions for $\mathcal{F}_{jmp}\,(i)$ are

$$\begin{aligned}\mathcal{F}_{jmp}\,(i) = &\sum_{t=0}^{min\left(p,[\frac{j-m}{2}]\right)} \frac{(2j-2t)!}{t!\,(j-t)!\,(j-m-2t)!2^{2j-2t}}\sin^{j-m-2t}(i)\\ &\times\sum_{s=0}^{m}\binom{m}{s}\cos^{s}(i)\sum_{c}\binom{j-m-2t+s}{c}\binom{m-s}{p-t-c}(-1)^{c-k}\ ,\end{aligned}$$

where the index c takes all values that do not nullify the binomial coefficients.

Finally, we do not give the general expression of the quantities $\mathcal{G}_{jpq}\,(e)$ since it is a long one and we rather limit to particular choices of the index q, as needed for the computation of (2.11). Setting $q=2p-j$, we obtain the expressions

$$\mathcal{G}_{jp(2p-j)}\,(e) = \frac{1}{(1-e^2)^{j-\frac{1}{2}}}\sum_{d=0}^{p'-1}\binom{j-1}{2d+j-2p'}\binom{2d+j-2p'}{d}\left(\frac{e}{2}\right)^{2d+j-2p'}\ ,$$

where

$$\begin{cases} p'=p & \text{per } p\le\frac{j}{2}\\ p'=j-p & \text{per } p\ge\frac{j}{2}\ .\end{cases}$$

References

[1] V. I. Arnold, *Proof of a Theorem by A.N. Kolmogorov on the invariance of quasi-periodic motions under small perturbations of the Hamiltonian,* Russ. Math. Surveys **18** (1963) 13-40

[2] G. Beutler, *Methods of Celestial Mechanics*, Volume I, Springer (2005)
[3] D. Brouwer, *Solution of the problem of artificial satellite theory without drag*, Astron. J. **64**, (1959) 378-397
[4] H. Cabral, C. Vidal, *Periodic solutions of symmetric perturbations of the Kepler problem*, J. Diff. Eq. **163** (2000) 76-88
[5] R. Calleja, A. Celletti, R. de la Llave, *A KAM theory for conformally symplectic systems: efficient algorithms and their validation*, J. Differential Equations **255**, n. 5 (2013) 978-1049
[6] A. Celletti, L. Chierchia L., *Rigorous estimates for a Computer-assisted KAM theory*, J. Math. Phys. **28** (1987) 2078-2086
[7] A. Celletti, C. Galeş, G. Pucacco, *Bifurcation of lunisolar secular resonances for space debris orbits*, SIAM J. Appl. Dyn. Syst. **15**, n. 3 (2016) 1352-1383
[8] A. Celletti, P. Negrini, *Non-integrability of the problem of motion around an oblate planet*, Celest. Mech. Dyn. Astr. **61** (1995) 253-260
[9] C.G. Chao, *Applied Orbit Perturbation and Maintenance*, Aerospace Press Series, AIAA, Reston, Virgina (2005)
[10] R. Cushman, *Reduction, Brouwer's Hamiltonian, and the critical inclination*, Celest. Mech. **31** (1983) 401-429
[11] D. del-Castillo-Negrete, J.M. Greene, P.J. Morrison, *Area preserving nontwist maps: periodic orbits and transition to chaos*, Physica D **91** (1996) 1-23
[12] A. Delshams, R. de la Llave, *KAM theory and a partial justification of Greene's criterion for non-twist maps*, SIAM J. Math. Anal. **31**, n.6 (2000) 1235-1269
[13] S.P. Diliberto, W.T. Kyner, R.B. Freund, *The Application of Surface Theory to the Study of Satellite Orbits*, Astr. J. **66** (1961) 118-128
[14] H. R. Dullin, J. M. Meiss, D. Sterling, *Generic Twistless Bifurcations*, Nonlinearity **13**, n. 1 (2001) 203-224
[15] A. Gonzalez-Enriquez, A. Haro, R. de la Llave, *Singularity theory for non-twist KAM tori*, Memoirs AMS **227**, n. 1067 (2014)
[16] M. Irigoyen, C. Simó, *Non integrability of the J_2 problem*, Celest. Mech. Dyn. Astr. **55** (1993) 281-287
[17] W.M. Kaula, *Theory of Satellite Geodesy*, Dover Publications (2000)
[18] W.T. Kyner, *Qualitative Properties of Orbits about an Oblate Planet*, Comm. Pure Appl. Math. **17** (1964) 227-236
[19] W.T. Kyner, *Rigorous and Formal Stability of Orbits About an Oblate Planet*, M. Am. Math. Soc. **81** (1968) 61-87
[20] A. N. Kolmogorov, *On the conservation of conditionally periodic motions under small perturbation of the Hamiltonian*, Dokl. Akad. Nauk. SSR **98** (1954) 527-530
[21] R. de la Llave, A. Gonzalez, A. Jorba, J. Villanueva, *KAM theory without action-angle variables*, Nonlinearity **18** (2005) 855-895
[22] J. Martinez Alfaro, *Collision orbits in the oblate planet problem*, Celest. Mech. **33** (1984) 375-383

[23] F. Mignard, *The evolution of the lunar orbit revisited. I*, The Moon and the Planets **20** (1979) 301-315

[24] F. Mignard, *The evolution of the lunar orbit revisited. II*, The Moon and the Planets **23** (1980) 185-201

[25] J. Moser, *On invariant curves of area–preserving mappings of an annulus*, Nach. Akad. Wiss. Göttingen, Math. Phys. Kl. II **1** (1962) 1-20

[26] E. Petrisor, *Reconnection scenarios and the threshold of reconnection in the dynamics of non-twist maps*, Chaos, Solitons and Fractals **14** (2002) 117-127

[27] C. Simó, *Invariant Curves of Analytic Perturbed Nontwist Area Preserving Maps*, Reg. Chaotic Dynamics **3** (1998) 180-195

[28] G. Stagika, S. Ichtiaroglou, *Twist and Non-twist Bifurcations in a System of Coupled Oscillators*, Cel. Mec. Din. Astr. **78** (2000) 151-160

[29] J.P. van der Weele, T.P. Valkering, *The birth process of periodic orbits in non-twist maps*, Physica A **169** (1990) 42-72

[30] J.P. van der Weele, T.P. Valkering, H.W. Capel, T. Post, *The birth of twin Poincaré-Birkhoff chains near 1:3 resonance*, Physica A **153** (1988) 283-294

[31] A. Wurm, A. Apte, K. Fuchss, P.J. Morrison, *Meanders and reconnection-collision sequences in the standard nontwist map*, Chaos **15** (2005) 1-13

Department of Mathematics, University of Rome Tor Vergata, Via della Ricerca Scientifica 1, 00133 Rome (Italy)
E-mail address: `celletti@mat.uniroma2.it`

Department of Mathematics, University of Rome Tor Vergata, Via della Ricerca Scientifica 1, 00133 Rome (Italy)
E-mail address: `f.paita@alice.it`

Department of Physics, University of Rome Tor Vergata, Via della Ricerca Scientifica 1, 00133 Rome (Italy)
E-mail address: `pucacco@roma2.infn.it`

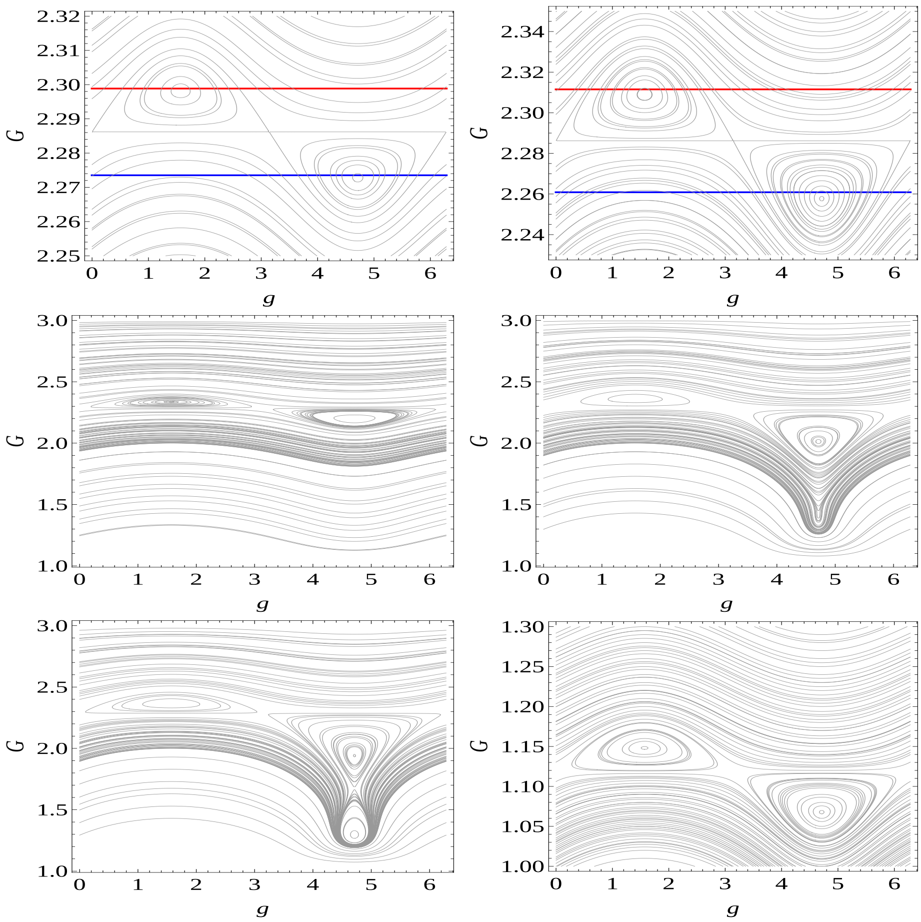

FIGURE 2. Contour plots for $\widetilde{L} = 3$, $G_0 = 2.8$, $J_2 = 10^{-2}$: top left $H = G_0 \sqrt{\frac{2}{15}}$, $J_3 = 10^{-3}$; top right $H = G_0 \sqrt{\frac{2}{15}}$, $J_3 = 2 \cdot 10^{-3}$; middle left $H = G_0 \sqrt{\frac{2}{15}}$, $J_3 = 5 \cdot 10^{-3}$; middle right $H = G_0 \sqrt{\frac{2}{15}}$, $J_3 = 8.83 \cdot 10^{-3}$; bottom left $H = G_0 \sqrt{\frac{2}{15}}$, $J_3 = 9.3 \cdot 10^{-3}$; bottom right $H = 0.5$, $J_3 = 10^{-3}$. The horizontal lines in the top panels represent the analytical estimates of the values of G corresponding to the equilibria.